

# Comparing Energy Consumption following Flight Pattern for Quadrotor

Sunho Jee\*, Hyunchan Cho\*★

## Abstract

Currently, many companies have succeeded in logistics delivery experiments utilizing drone and report it. When a drone is used commercially, long-term flight is an important performance that a drone should have. However, unlike vehicles operated on the ground, drone is a vehicle that continues to consume energy when maintaining the current altitude or moving to the destination. Therefore, the drones can fly for a long time as the capacity of the battery is large, but the batteries with large capacity are restricted by heavy weight and it acts as a limiting factor in a commercial use. To address this issue, we attempt to compare how far we can fly than forward flight based on the flight pattern with the same energy consumption condition. In this paper, the comparison of energy consumption was performed in three flight pattern, forward flight without altitude change and forward flight with altitude change, by computer simulation and it shows the increasing of flight distances when the quadrotor fly with altitude change from high altitude to low altitude..lb

*Key words: drone flight, energy consumption, flight pattern, quadrotor, unmanned aerial vehicle*

## 1. Introduction

Unattended aircraft (unmanned aircraft) are aircraft that fly along planned routes, recognize and analyze their environment, and autonomous flight related applications such as traffic monitoring, human life, geology and mining,

When drones are used, they often collide with obstacles or unexpected accidents during takeoff and landing. To address this problem, many types of drones have been developed and studied focusing on flight control techniques such as hovering, vertical takeoff and landing, and avoidance of obstacles using many kinds of sensors and vision. In particular, the type of

multi-rotor drones with BLDC motors and propellers are preferred because they can replace people who work in dangerous environments at low cost and compact sizes. In order to control the rotational motion of these multi-rotor types of unmanned aircraft, various approaches have been studied using fuzzy logic, sliding mode control, and predictive control. [1]-[4]

The algorithms for path-following also studied using integral predictive and nonlinear robust control strategy, closed-loop control with internal model control position sensor, and etc. [5]-[6] Through various researches on unmanned aerial vehicles in the form of multi-rotor, drones are actively being used to provide aerial photography

---

\* School of Electrical, Electronics and Communication Engineering, KOREATECH

★ Corresponding author

E-mail : cholab@koreatech.ac.kr, Tel : +82-41-560-1170

※ Acknowledgment

This work was supported by 2017 Education and Research promotion program funded by KOREATECH

Manuscript received Sep. 7, 2018; revised Sep. 18, 2018; accepted Sep. 19, 2018;

This is an Open-Access article distributed under the terms of the Creative Commons Attribution Non-Commercial License (<http://creativecommons.org/licenses/by-nc/3.0>) which permits unrestricted non-commercial use, distribution, and reproduction in any medium, provided the original work is properly cited.

and broadcasting images and FedEx, DHL, Amazon, and others successfully announced their logistics delivery experiment using the drones. [7]–[8]

However, as many electronic devices are added to drones that use batteries, flight time has gradually decreased, and this is a factor limiting commercial use. If battery capacity is increased to increase flight time, this will be linked again to increase weight of drones, which will affect flight time. Therefore, research was carried out to solve minimum route problem for commercial use of drone flying using batteries.

Because drones have small capacity and limited flight time, only small packages can be moved by route. Due to these drone characteristics, the flight time limit of the battery was approached by minimizing the flight path including the warehouse and mainly TSP study was conducted. [9]–[11] A drone is an airplane that determines its flight speed and direction of flight depending on the magnitude of thrust and direction of thrust. However, most studies assume that the path for travel is to travel straight in flight.

In this paper, we simulate about different flight pattern that have same final point for comparing power consumption by comparing rotor speed of each cases.

## II. Mathematical Modeling

### 2.1 Dynamics of quadrotor

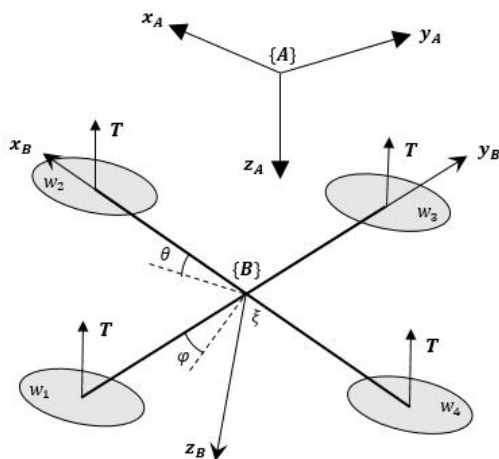


Fig. 1. Physical model of quadrotor.

Fig. 1 shows a quad-rotor type non-conductor with all of its thrust propellers aligned in one direction and {A} means inertia frame and {B} means body frame.

Drones operate in an aligned direction of the propeller and have four inputs as they can be rotated in three directions. At this time, the drone has a total of six degrees of freedom since it can move and rotate in three axes of  $x$ ,  $y$ ,  $z$  in three dimensional space, but since the control input is the thrust forces of four rotors, that is, four degrees of freedom, it has an under-actuation characteristic that there are less degree of freedom of control inputs than the degree of freedom of the system. This characteristic makes it difficult to control quad-rotor type drones. These dynamics of quad-rotors have been studied in detail by several groups [12–14] and using the Newton equation as shown in (1).

$$\begin{cases} m\ddot{x} = -T \text{Re}_3^B + mg e_3^I + f_a \\ J\dot{\Omega} + \Omega_x J\Omega = \tau + \tau_a \\ \dot{R} = S(\Omega)R \end{cases} \quad (1)$$

where  $m$  means drone weight,  $J \in \mathbb{R}^{3 \times 3}$  means rotational inertia,  $T$  means the thrust force from all propellers,  $\tau$  means total torque from all propellers,  $x$  means position vector of drone,  $\Omega$  means angular velocity of quadrotor in body frame. The matrix  $R \in SO(3)$  means the rotational transformation from inertial frame to body frame,  $g$  means gravity,  $e_3 = (0, 0, 1)$  means unit vector indicating  $z$ -direction and indicates that thrust force and gravity act on respectively the direction of the drone and the direction of the coordinate system.  $f_a$  and  $\tau_a$  are aerodynamic factors resulting from the movement of the drone and it is often assumed to be simplified or very small at speeds above 10 m/s. [15]

The total thrust and torque produced by the four rotors are expressed in  $T$  and  $\tau$ , and can

be obtained using the following models.

$$T = k \sum_{i=1}^4 w_i^2 \tag{2}$$

The relationship of angular speed, thrust force and torque of each propeller for control inputs is as follows.

$$\begin{bmatrix} T \\ \tau_1 \\ \tau_2 \\ \tau_3 \end{bmatrix} = \begin{bmatrix} k & k & k & k \\ 0 & L & 0 & -L \\ L & 0 & -L & 0 \\ -b & b & -b & b \end{bmatrix} \begin{bmatrix} w_1^2 \\ w_2^2 \\ w_3^2 \\ w_4^2 \end{bmatrix} \tag{3}$$

where  $k, b$  means the positive proportionality constants that determine the relationship between propeller speed, thrust force and rotational moment,  $L$  means distance between propeller and drone center,  $\tau_i$  means torque of roll, pitch, yaw directions,  $w_i$  means each propeller's rotation speed.

### 2.2 Motor energy consumption

Although the components that use power in quadrotors are motors, ESC, and several types of sensors, the energy consumption of motors is significantly higher than that of electronic devices, so only the energy consumption of motors is considered.

The model of brushless DC motor using battery is considered to be the energy consumed in resistive and inductive windings and the energy required to overcome internal and load friction. The instantaneous current  $i(t)$  and the voltage across the motor  $v(t)$  is given as follows. [16-17]

$$v(t) = Ri(t) + K_E w(t) + L \frac{di(t)}{dt} \tag{4}$$

$$i(t) = \frac{1}{K_T} [T_f + T_L(w(t)) + D_f w(t) + (J_m + J_L) \frac{dw(t)}{dt}] \tag{5}$$

where  $w(t)$  describes the angular velocity of the motor shaft,  $K_T$  is the torque constant of the

motor,  $T_f$  is the motor friction torque,  $T_L(w(t))$  is the speed-dependent load friction torque which results from propeller drag,  $D_f$  is the viscous damping coefficient of the motor,  $J_m, J_L$  are the motor and load moments of inertia, respectively.  $R$  is the resistance and  $K_E$  is the voltage constant of the motor. Then the energy consumption is given as follows. In a brushless DC motor  $T_f$  is small, usually only due to bearing drag, the viscous damping coefficient is also very small, and both items can usually be ignored in dynamic performance calculations. [18]

The energy consumed by the quadrotor between the initial time  $t_0$  and the end time  $t_f$  are as follows.

$$E = \int_{t_0}^{t_f} \sum_{j=1}^4 \begin{bmatrix} c_1 + c_2 w_j(t) + c_3 w_j^2(t) \\ + c_4 w_j^3(t) + c_5 w_j^4(t) \\ + c_6 \dot{w}_j(t) + c_7 \dot{w}_j^2(t) + \\ c_8 w_j(t) \dot{w}_j^2(t) + c_9 w_j^2(t) \dot{w}_j(t) \end{bmatrix} dt \tag{6}$$

$$E_R = \int_{t_0}^{t_f} \sum_{j=1}^4 \begin{bmatrix} c_1 + c_2 w_j(t) + c_3 w_j^2(t) + \\ c_4 w_j^3(t) + c_5 w_j^4(t) + c_7 \dot{w}_j^2(t) \end{bmatrix} dt \tag{7}$$

where  $\dot{w}_j(t)$  is the angular acceleration of motor  $j$ , and  $c_1, c_2, \dots, c_9$  are constants depending on the parameters of the motors and on the geometry of the propeller.

### III. Flight pattern with maximum thrust

If a destination can't be observed at the starting point, it is not possible to manually control the quadrotor and arrive at the destination due to the pilot's limited visibility. For this reason, many algorithms have been studied to create unmanned flight paths, but networks that focus only on flight points or flight distances without considering flight patterns

or flight altitude changes. However, in order to stabilize unmanned flights and reduce power consumption, a change in height is considered even though it is a straight line connecting the points with the points.

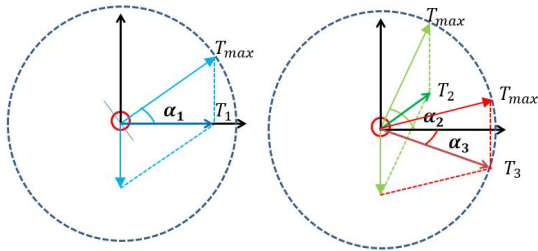


Fig. 2. Vectors of several flight directions and magnitudes generated along the direction in which thrust applied.

When the drone generates maximum thrust, Fig.2 shows the direction and magnitude of the force generated by the direction of the thrust. and it shows that even though maximum thrust is generated in a direction perpendicular to the drone, different forces are occurring depending on the attitude of drone. Following the attitude of the drone,  $T_1$  is generated in a straight direction,  $T_2$  is generated upward and  $T_3$  is generated downward direction with maximum thrust. It shows the different magnitude following acting angles of thrust even though all pattern has maximum thrust.

At this time, each generated vector has relationship as  $T_2 < T_1 < T_3$ . This means that there is a pattern of paths that can fly further with the same energy consumption. In order to apply this glide pattern, the flight height to the destination must be determined at the beginning of the flight and This height must be set to compensate for the energy consumption used when the drone is climbing in the X-Axis direction, and as a result, the total energy consumption on arrival at the destination should be less than for the straight path flight.

Drones can be expressed as in equation (1) under Newton's second law of motion, based on classical mechanics. In both cases of vertical

climb or a straight flight at a given altitude, releasing the expression based on equation (1) will cause air resistance to no longer accelerate and reach the speed limit. Calculate this speed limit as the maximum attainable speed in a climb or a straight flight as follows.

$$v = \sqrt{\frac{2mg_0}{\rho C_D A_{eff}}} \times \sqrt{T_r - 1} \tag{8}$$

$$v = \sqrt[4]{T_r^4 - T_r^2} \times \sqrt{\frac{2mg_0}{\rho C_D A_{eff}}} \tag{9}$$

The maximum rising and flight speed can be expressed by (8) and (9).  $T_r$  is ratio with hovering thrust,  $g_0$  is gravity,  $\rho$  is density of air,  $c_D$  is drag coefficient and  $A_{eff}$  is effective area of the drone.

### IV. Simulations

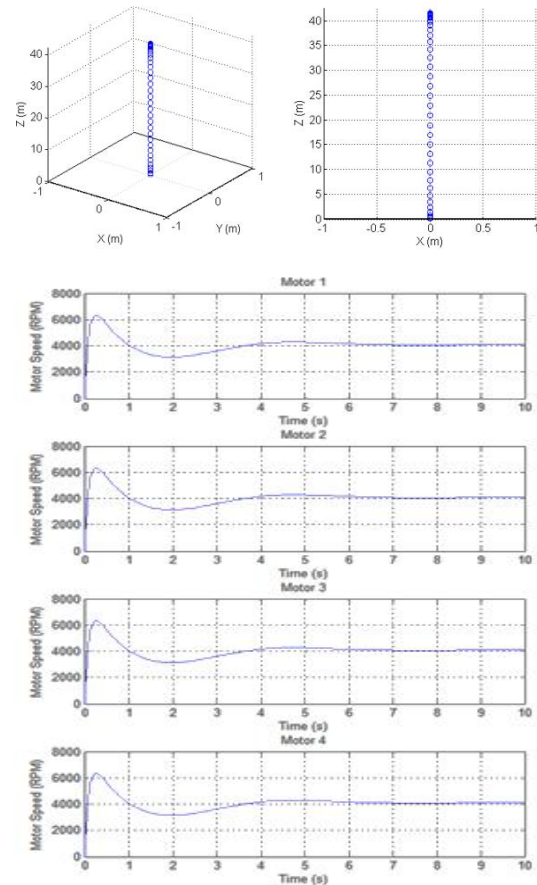
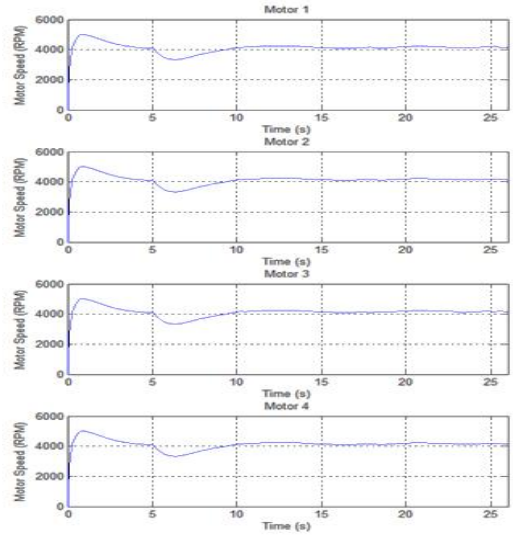
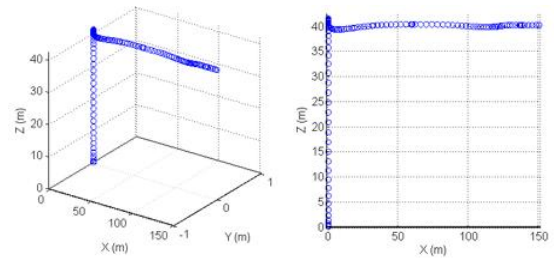


Fig. 3. Simulation results of hovering case.

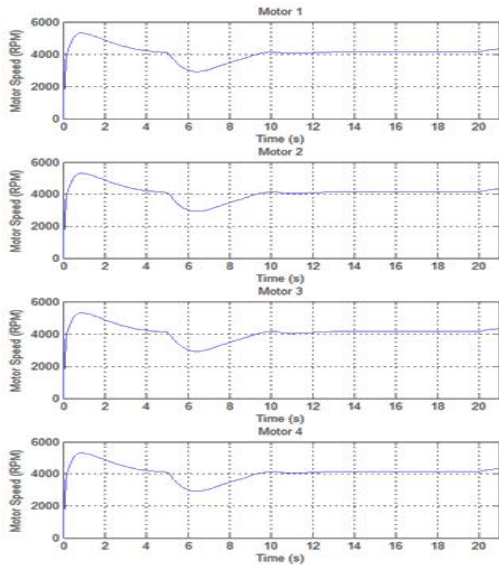
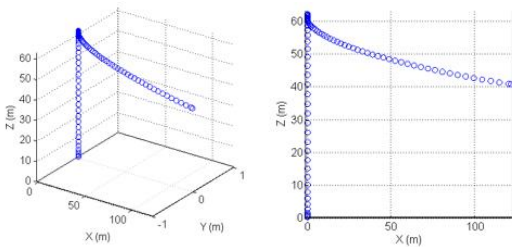
With the maximum thrust, we make three flight pattern with just changing attitude and use PID controller for following path. The rpm when the quadrotor hovers in [0m, 0m, 40m] is measured to compare the rotational speed of the motor of each path and the power consumption.

Fig. 3 shows the result of hovering case, all motors have MH = 4178 rpm to hover. Each initial positions set [0m, 0m, 60m], [0m, 0m, 40m], [0m, 0m, 20m] and final position set [150m, 0m, 40m] for comparing motor speed. At this time, the quadrotor start flight after hovering at each positions during 10 seconds.

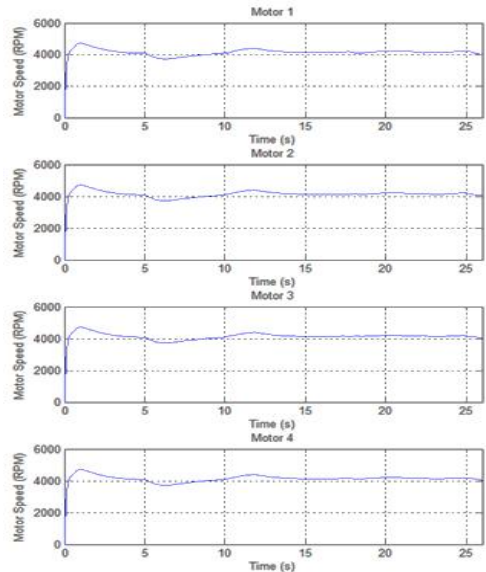
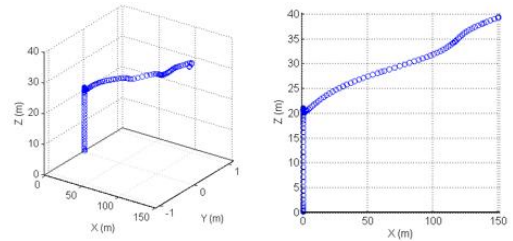
Fig. 4(a), (b), (c) show the result of motor speed as each flight pattern. When the quadrotor fly x direction, all point has same flight speed with maximum for each cases. Table 1 shows each motor speed of each flight pattern.



(b) Case of forward flight



(a) Case of downward flight



(c) Case of upward flight

Fig. 4. Simulation results of height changing flight

Table 1. Each motor speed of Each flight pattern

Motor#n	Downward	Forward	Upward
M1	4055rpm	4199rpm	4315rpm
M2	4048rpm	4193rpm	4309rpm
M3	4043rpm	4187rpm	4303rpm
M4	4048rpm	4193rpm	4309rpm

In Fig. 4(a), the drone starts higher altitude than final point and it shows each motor speed as M1=4055rpm, M2=M4=4048rpm, M3=4043rpm. All motors are rotated slower than MH = 4178rpm, motor 1 is faster than motor 3 for downward flight. At final point, all motors are converged to 4178rpm.

In Fig. 4(b), the drone starts same altitude of final point and it shows each motor speed as M1=4055rpm, M2=M4=4048rpm, M3=4043rpm. It seems similar to the downward flight pattern but all motors are faster than MH = 4178rpm.

In Fig. 4(c), the drone starts lower altitude than final point and it shows each motor as M1=4055rpm, M2=M4=4048rpm, M3=4043rpm. It also seems similar to the downward and forward flight pattern but all motors are faster than MH = 4178rpm.

## V. Conclusion

Drone has same power consumption for hovering even though the altitude is different because of its characteristic. The power consumption of downward is lower than hovering and the power consumption of upward and forward are higher than hovering. The simulation shows comparing with hovering case that the motor speed of drone is different according to altitude of initial position when the drone fly to an arbitrary position and it shows the result as  $P_{downward} < P_{hovering} < P_{forward} < P_{upward}$ . So, it is necessary to consider changing power consumption by the previous altitude for path generation for minimizing power consumptions.

Future work will consider develop algorithm

for path generation with changing altitude. Additionally, we also consider develop algorithm for obstacle avoidance and we intend to investigate the performance of the proposed algorithm in a hardware implementation.

## References

- [1] Omari, S., Hua, M. D., Ducard, G., & Hamel, T. "Hardware and software architecture for nonlinear control of multirotor helicopters.," *IEEE/ASME Transactions On Mechatronics*, vol.18, no.6, pp.1724-1736, 2013. DOI:10.1109/TMECH.2013.2274558
- [2] Razinkova, A., Kang, B. J., Cho, H. C., Jeon, H. T., "Constant altitude flight control for quadrotor UAVs with dynamic feedforward compensation," *International journal of fuzzy logic and intelligent systems*, vol.14, no.1, pp.26-33, 2014. DOI:10.5391/IJFIS.2014.14.1.26
- [3] Bouadi, H., Bouchoucha, M., & Tadjine, M., "Sliding mode control based on backstepping approach for an UAV type-quadrotor," *World Academy of Science, Engineering and Technology*, vol.26, no.5, pp.22-27, Jan. 2007.
- [4] Kang, Y., & Hedrick, J. K., "Linear tracking for a fixed-wing UAV using nonlinear model predictive control," *IEEE Transactions on Control Systems Technology*, vol.17, no.5, pp.1202-1210, 2009. DOI:10.1999/1307-6892/11524
- [5] Raffo, G. V., Ortega, M. G., & Rubio, F. R., "An integral predictive/nonlinear  $H^\infty$  control structure for a quadrotor helicopter," *Automatica*, vol.46, pp.29-39, 2009. DOI:10.1016/j.automatica.2009.10.018
- [6] Hernandez, A., Copot, C., De Keyser, R., Vlas, T., Nascu, I., "Identification and path following control of an AR. Drone quadrotor.," *2013 17th International Conference on System Theory, Control and Computing(ICSTCC)*, 2013, pp.583-588. DOI:10.1109/ICSTCC.2013.6689022
- [7] D. Gross., "Amazon's drone delivery: How would it work?," <https://www.cnn.com/> (URL)

- [8] A.C. Madrigal., "Inside Google's secret drone delivery program," <https://www.theatlantic.com/> (URL)
- [9] Dorling, K., Heinrichs, J., Messier, G. G., Magierowski, S., "Vehicle routing problems for drone delivery," *IEEE Transactions on Systems, Man, and Cybernetics: Systems*, vol.47, pp.70-85, 2016. DOI:10.1109/TSMC.2016.2582745
- [10] Murray, C. C., Chu, A. G., "The flying sidekick traveling salesman problem: Optimization of drone-assisted parcel delivery," *Transportation Research Part C: Emerging Technologies*, vol. 54, pp.86-109, 2015. DOI:10.1016/j.trc.2015.03.005
- [11] Erdoğan, S., Miller-Hooks, E., "A green vehicle routing problem," *Transportation Research Part E: Logistics and Transportation Review*, vol.48, no.1, pp.100-114, 2012. DOI:10.1016/j.tre.2011.08.001
- [12] Bouabdallah, S., Murrieri, P., Siegwart, R., "Design and control of an indoor micro quadrotor," *IEEE International Conference on Robotics and Automation(ICRA2004)*, 2004, pp.4393-4398. DOI:10.1109/ROBOT.2004.1302409
- [13] McKerrow, P., "Modelling the Draganflyer four-rotor helicopter," *IEEE International Conference on Robotics and Automation(ICRA2004)*, 2004, pp. 3596-3601.
- [14] Bangura, M., & Mahony, R., "Nonlinear dynamic modeling for high performance control of a quadrotor," *Australasian conference on robotics and automation(ACRA2012)*, pp.1-10, 2004. DOI:10.1109/ROBOT.2004.1308810
- [15] Gandolfo, D. C., Salinas, L. R., Brandão, A., Toibero, J. M., "Stable path-following control for a quadrotor helicopter considering energy consumption," *IEEE Transactions on Control Systems Technology*, vol.25, no.4, pp.1423-1430, 2017. DOI:10.1109/TCST.2016.2601288
- [16] Carrillo, L. R. G., López, A. E. D., Lozano, R., Pégard, C., *Quad rotorcraft control: vision-based hovering and navigation.*, Springer Science & Business Media, 2013.
- [17] Mahony, R., Kumar, V., & Corke, P.,

- "Multirotor aerial vehicles: Modeling, estimation, and control of quadrotor," *IEEE Robotics & Automation Magazine*, vol.19, no.3, pp.20-32, 2012. DOI:10.1109/MRA.2012.2206474
- [18] Morbidi, F., Cano, R., & Lara, D., "Minimum-energy path generation for a quadrotor UAV," *IEEE International Conference on Robotics and Automation(ICRA2016)*, 2016, pp.1492-1498. DOI:10.1109/ICRA.2016.7487285

## BIOGRAPHY

### Sunho Jee (Member)



2009 : BS degree in Electronic Engineering, KOREATECH.  
 2011 : MS degree in Electronic Engineering, KOREATECH.  
 2013~present : Ph.D. student, School of Electrical, Electronics and Communication Engineering, KOREATECH.

### Hyunchan Cho (Member)



1991 : PhD degree in Electronics Engineering, Chung-Ang University.  
 1991~present : Professor, School of Electrical, Electronics and Communication Engineering, KOREATECH.